References and Notes

(1) Miller, L. L.; Van de Mark, M. R. *J. Am. Chem. Soc.* **1978,** 100, 639. *J. Electroanal. Chem.* **1978,** *88,* 437.
(2) Van de Mark, M. R.; Miller, L. L. *J. Am. Chem. Soc.* **1978,** 100, 3225.
(3) Merz, A.; Bard, A. J. *J. Am. Chem. Soc.* **1978,** 100, 3222.
(4) Itaya, K.; Bard, A. J. *Anal. Chem.* **1978,** 51, 1487.
(5) Oyama, N.; Anson, F. C. *J. Am. Chem. Soc.* **1979,** *101,* 739.
(6) Dobelhofer, K.; Nöete, D.; Ulstrup, J. *Ber. Bunsenges. Phys. Chem.* **1978,** *82,* 403.
(7) Nowak, R.; Schultz, F. A.; Umaña, M.; Abruña, H.; Murray, R. W. *J. Electroanal. Chem.* **1978,** *94,* 219.
(8) Rafikov, S. R.; Pavlova, S. A.; Tverdokhlebova, I. I. "Determination of Molecular Weights and Polydispersity of High Polymers", Daniel Davey: New York, 1964; Chapter IX.
(9) Mukaida, H.; Okuno, H.; Ishimori, T. *Nippon Kagaku Zasshi* **1965,** 86, 56.
(10) Evans, J. F., Kuwana, T. *Anal. Chem.* **1977,** *49,* 1632.
(11) Oyama, N.; Brown, A. P.; Anson, F. C. *J. Electroanal. Chem.* **1978,** 87, 435.
(12) Brown, A. P.; Koval, C.; Anson, F. C. *J. Electroanal. Chem.* **1976,** *72,* 379.
(13) Brown, A. P.; Anson, F. C. *J. Electroanal. Chem.* **1977,** *83,* 203.
(14) Koval, C. A.; Anson, F. C. *Anal. Chem.,* **1978,** *50,* 223.
(15) Matsubara, T.; Creutz, C. *J. Am. Chem. Soc.* **1978,** *100,* 6255.
(16) Oyama, N.; Anson, F. C. *J. Electroanal. Chem.* **1978,** *88,* 289.
(17) Laviron, E. *J. Electroanal. Chem.* **1972,** *39,* 1.
(18) Matsubara, T.; Creutz, C., submitted for publication in *J. Am. Chem. Soc.*
(19) Shepherd, R. E.; Taube, H. *Inorg. Chem.* **1973,** *12,* 1392.
(20) Oyama, N.; Anson, F. C. *J. Am. Chem. Soc.,* **1979,** *101,* 1634.
(21) Shimizu, K.; Matsubara, T.; Sato, G. P. *Bull. Chem. Soc. Jpn.* **1974,** *47,* 1651.
(22) Wrighton, M. S.; Palazzotto, M. C.; Bocarsly, A. B.; Bolts, J. M.; Fischer, A. B.; Nadjo, L. *J. Am. Chem. Soc.* **1978,** *100,* 7264.
(23) Brown, A. P.; Anson, F. C. *J. Electroanal. Chem.* **1978,** *92,* 133.
(24) Oyama, N.; Anson, F. C. Unpublished experiments.
(25) Andrieux, C. P.; Saveant, J. M. *J. Electroanal. Chem.* **1978,** *93,* 163.

M3L9(ligand) Complexes

Birgitte E. R. Schilling and Roald Hoffmann*

Contribution from the Department of Chemistry, Cornell University, Ithaca, New York 14853. Received October 5, 1978

Abstract: The frontier orbitals of an M₃(CO)₉ unit are constructed from three M(CO)₃ pieces or by removing three ligands from a D_{3h} M₃(CO)₁₂. They consist of a relatively low-lying Walsh-like set 1a₁ + 1e and a higher cyclopropenium-like 2a₁ + 2e. The latter are empty for a d^8 M. These orbitals are used to analyze the electronic and geometrical structure of M₃L₉(ligand) complexes where the ligand is CO, S, (CO)₂, S₂, CR, CCH₂⁺, ethylene, acetylene, or acyclic and cyclic polyenes. In the case of (CO)₃Co₃CCH₂⁺ the symmetrically topped structure is not a local energy minimum, but instead there are three equivalent unsymmetrical structures of a complexed ethylidene type.

The rich and beautiful chemistry of metal clusters is unfolding only now.[1,2] Perhaps its most highly developed aspect is the reactivity of trinuclear compounds. Both structural data and reactivity studies cover a wide range of such complexes including systems with both bridging and terminal carbonyls or hydrides or highly complicated molecules where the ligand no longer can be separated from the cluster unit.

Following earlier work on binuclear complexes,[3] we are interested in building a detailed understanding of the electronic determinants of structure and reactivity in these molecules. In this study we concentrate on complexes of the symmetric M₃L₉ unit. The ligands which bond to this fragment, commonly organic systems, can be divided into several groups. An example of a ligand bonded through a single atom is shown in **1**.[4] Unsaturated π-bonded ligands are found, such as the iron acetylene compound **2**,[5] or cyclic systems of the type **3**.[6]

1	**2**	**3**
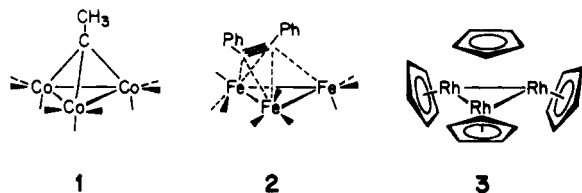
The basic unit is M₃(CO)₉ or variations thereof, such as M₃Cp₃. We will construct the frontier orbitals of this fragment and then interact it with a range of organic and inorganic caps. Symmetry based arguments will be supported by extended Hückel calculations for M = Fe, with details given in the Appendix.

Orbitals of the Fe₃(CO)₉ Fragment

The orbitals of a C_{3v} M₃(CO)₉ fragment may be constructed by interacting three M(CO)₃ groups or by stripping three carbonyls from a D_{3h} M₃(CO)₁₂. The former procedure gives more detail, while the latter provides a pedagogically simple entry into the problem. We will proceed with both approaches, starting with M₃(CO)₁₂ first.

It is well-known that only Ru₃(CO)₁₂ and Os₃(CO)₁₂ have a D_{3h} structure,[7] while Fe₃(CO)₁₂ has two bridging carbonyls in a C_{2v} geometry.[8] Also these molecules are fluxional in character.[9] Nevertheless, for the sake of simplicity we aim for the orbitals of the C_{3v} M₃(CO)₉ and so begin with a D_{3h} M₃(CO)₁₂.

4

A D_{3h} M₃(CO)₁₂ is a "saturated" electron precise molecule, the inorganic analogue of a cyclopropane. It may be assembled from three octahedral fragment M(CO)₄ units. The orbitals of such a fragment[10] are shown below. Above the remnants of the octahedral t₂g set there are two hybrids pointing toward the missing octahedral sites, a₁ and b₂. These are analogous to the σ and p orbitals, respectively, of a methylene.[11] The Fe(CO)₄ and CH₂ fragments are isolobal,[12] each with two electrons in these upper frontier orbitals. Thus the formation of a symmetric trimer Fe₃(CO)₁₂, Figure 1, is analogous to the formation of cyclopropane from three methylenes.[13] While the three t₂g levels interact little, to generate a low-lying cluster of nine orbitals, all filled, the upper b₂ + a₁ set interacts greatly to generate a Walsh-like set[13] of orbitals—1e′ and 1a₂′ from b₂, 1a₁′ and 2e′ from a₁. This picture has been constructed earlier.[14] The main difference from cyclopropane is that in the latter the e′ set derived from the peripheral orbitals is at higher
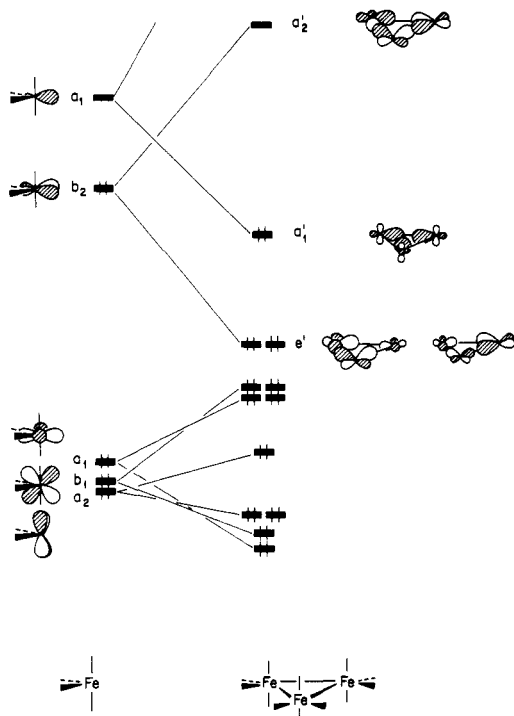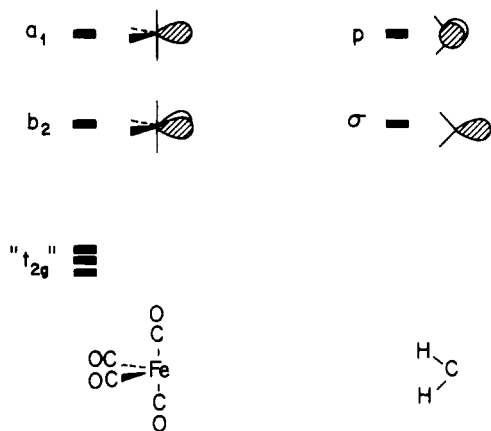
Figure 1. The orbitals of $Fe_3(CO)_{12}$ built up from three $Fe(CO)_4$ fragments.

energy than the a', while in $M_3(CO)_{12}$ this order is reversed. This is a consequence of the relative ordering in the monomer fragment, b_2 below a_1 in $M(CO)_4$, but σ below p in CH_2. The $M_3(CO)_{12}$ ordering of Walsh orbitals, $1e'$ below $1a_1'$, is confirmed by photoelectron studies on the Ru and Os com-

pounds,[15] and is consistent with the electronic spectrum of the trinuclear complexes.[14b]

In $M_3(CO)_{12}$ (M = Fe, Ru, Os) the available electrons just fill $1e'$ and $1a_1'$, hence the direct analogy to cyclopropane. If three axial carbonyls are removed there is a slight destabilizing effect on some of the filled oribitals, but the primary new feature is the appearance of three low-lying acceptor orbitals. These may be thought of as coming from the localized hybrid set shown in **5**, whose symmetry-adapted equivalent is a a_1' +

5
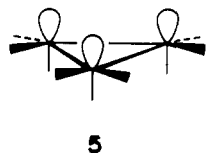
e' set. These cyclopropenium-type orbitals are ideally set up to interact with a capping ligand.
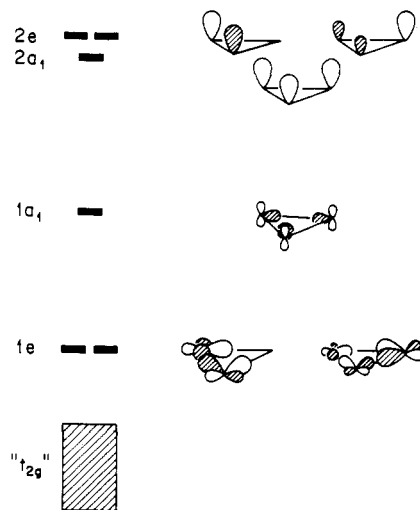

Figure 2. Schematic representation of the orbitals of $Fe_3(CO)_9$. Three Walsh type orbitals are below the a_1 and e combinations of the hybrid orbitals.

The qualitative picture that emerges for $M_3(CO)_9$ is summarized in Figure 2. Above a nest of nine "t_{2g}" levels there are three Walsh-type orbitals, $1a_1$ + $1e$. Still higher, vacant for M = Fe, Ru, Os, is a set of three excellent acceptor orbitals, $2a_1$ + $2e$. A d^8 $M_3(CO)_9$ fragment is like $C_3H_3^{3+}$, while for M having nine d electrons it is like $C_3H_3^{3+}$, while for M having nine d electrons it is like C_3H_3.

For a more detailed picture we return to the alternative construction from the equally well-known $M(CO)_3$ fragment orbitals.[9,16] In a C_{3v} geometry the orbitals emerge qualitatively as shown in **6**—a t_{2g} set below and a set of three orbitals above,

6
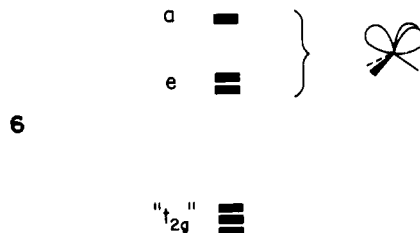
the delocalized equivalent of three hybrids pointing toward the vacant octahedral sites. But neither the C_{3v} geometry nor the coordinate system implicit in **6** is quite appropriate to the eventual trimer configuration. The fragment C_{3v} geometry needs to be lowered to C_s, one C–M–C angle 115.2°, the others 90°. This does not cause a serious perturbation of the $M(CO)_3$ levels, but does split the degeneracy of any e set. A coordinate system that better anticipates the trimer is that illustrated in **7**.

7
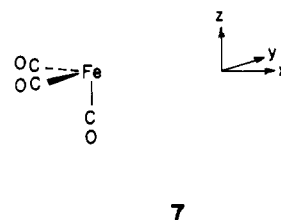
The monomer orbitals are shown schematically at the left side of Figure 3. In the new coordinate system the "t_{2g}" set is primarily $x^2 - y^2$, xz, and yz in character, while the upper e set has split into a symmetric, mainly z^2, and an antisymmetric, mainly xy, component. The topmost orbital is still very much oriented along the pseudo-threefold axis, being a mixture of s, p, and z^2.

When three $Fe(CO)_3$ fragments are joined together in a

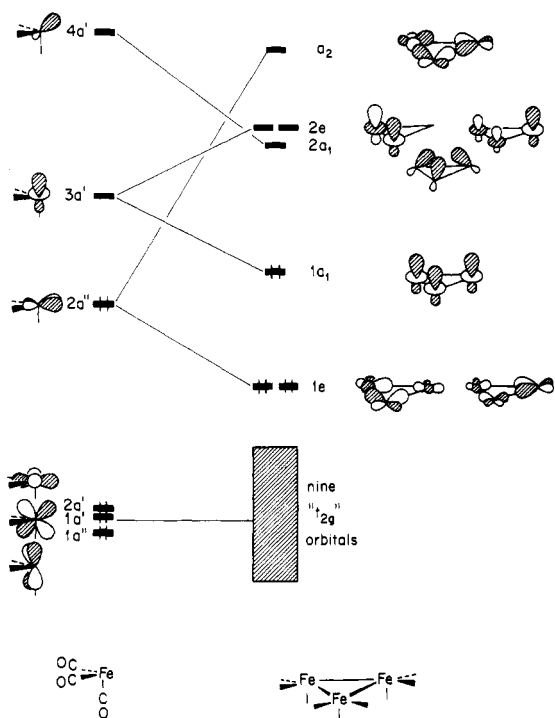**Figure 3.** Orbital scheme for $Fe_3(CO)_9$ generated from three $Fe(CO)_3$ fragments.

triangle, each triplet of identical MOs interacts to form an e set and an a_1 or a_2 orbital in the new C_{3v} symmetry. The lower three "t_{2g}" orbitals split up to form a broad cluster of nine molecular orbitals, all filled in the iron system. They are all close in energy and lower lying, and will therefore not behave as valence orbitals or participate strongly in bonding to additional ligands.

The MOs of interest from a bonding perspective are those descended from the higher three orbitals of the monomer. The hybrid orbital, the $4a'$ in the interaction diagram in Figure 3, will give a bonding a_1 orbital, stabilized greatly, and an antiboding e set, which will be too high in energy to be involved in bonding. The antisymmetric $2a''$ is mainly xy, hybridized toward the missing sites of the octahedron. When the metal triangle is constructed, the metal–metal bonds are formed close to the original octahedral sites, the 60° angle being somewhat smaller than the 90° of the octahedron. The overlap between the metals due to these orbitals is thus excellent, enhanced by both the very good directionality of the orbitals and a favorable hybridization. The splitting between the bonding a set and the antibonding a_2 is therefore large. The resulting $1e$ orbitals which are metal–metal bonding, filled in the iron system, and the empty a_2 are, however, primarily disposed in the metal plane. Therefore, they are not expected to interact strongly with ligands above the metal base. Later we will see that this is not true when the ligands enter close to the base and have appropriate matching nodal properties.

The MOs that will be most strongly involved in bonding to additional ligands are those descended from the z^2 ($3a'$) of $Fe(CO)_3$ and the in-phase combination of the hybrid ($4a'$) orbitals. The bonding combination of the z^2 will be of a_1 symmetry and lowered in energy. In the iron system this MO, the $1a_1$ in Figure 3, will be the highest occupied MO. The $2e$ set will be metal–metal antibonding and is found above the bonding hybrid $2a_1$. The pertinent valence orbitals are thus sets of three filled and three empty orbitals, just as we derived earlier. Plots of these MOs are shown in Figure 4. The plane of plotting has been chosen so as to best represent the character of the orbitals. The MOs of a_1 symmetry and the symmetric partner of the upper e set, $2e_s$, are shown in a plane containing
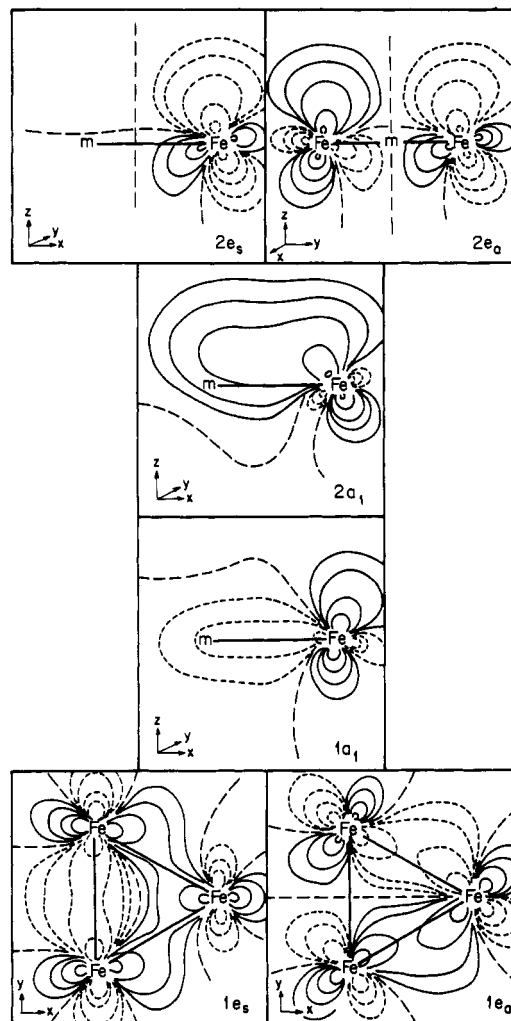

Figure 4. Contour plots of the valence orbitals of $Fe_3(CO)_9$ showing only the metal part. The a_1 orbitals and $2e_s$ are plotted in the xz plane, m indicating the midpoint of a metal–metal bond. $2e_a$ is in the yz plane and $1e$ is shown in the xy plane. The contour values are 0.2, 0.1, 0.05, and 0.025 with dotted lines indicating negative values. The dashed lines represent nodes.

one metal and bisecting a metal–metal bond. The $2e_a$ similarly has the plane perpendicular to the metal base, but shows a slice along a bond through two metals to illustrate the antibonding character of this MO. The plots of the lower e set, $1e$, are shown in the plane of the metal triangle, the area of largest electron density for this degenerate set.

Filled are the $1e$ set descended from monomer xy, concentrated in the plane of the metals, and the $1a_1$ consisting of z^2 on the metals. This latter orbital extends outward from the metal base, but is tilted somewhat. This results in poor overlap with ligands centered above the center of the metal cluster. The node of the z^2 is directed toward a point above the center of the triangle, as shown in the plot in Figure 4, such that this MO has no or only very low electron density above the midpoint of the cluster.

The acceptor orbitals of the metal cluster are the $2a_1$ and the $2e$ set. Note from Figure 4 the effective directionality of these orbitals. The six electron donors needed to satisfy the electronic demands of the iron cluster have just these three empty low-lying MOs to interact with. When the metal is cobalt, as is the case for several of the systems of interest, three more electrons, one per metal, have been added. Thus only three additional electrons are needed to satisfy the cluster.

We proceed to use the M_3L_9 fragment orbitals in the analysis of the electronic and geometrical structure of complexes

containing that unit. Several of the compounds available contain bridging hydrides, whose precise position has been established with more or less certainty. Rather than recalculate the orbitals of the hydride-containing fragment (which we will do someday) we resort to the approximation of thinking about these as protonated clusters, and use in our thinking the unprotonated cluster with the appropriate electron count. For instance, $H_2Os_3(CO)_9CCH_2$ will be analyzed as $Os_3(CO)_9$-CCH_2^{2-}.

Ligands Which Bond through One Atom

Complexes of a triangle of cobalts with nine terminal carbonyls and alkyl groups bound to a single carbon sitting above the center of the metal triangle, **8**, are numerous and a host of

8
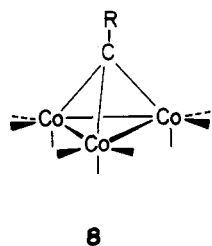
crystal structures are known.[1d] These cover simple alkyls like methyl, ethyl, or more complicated systems,[17] as well as alkyl groups bridging two or more three-metal systems.[18] We shall here restrict ourselves to the analysis of the basic bonding relationship between the carbon system and the metal base, using a C-H group as model for the more general C-R ligand.

In a simple hybrid picture the C-H group has three hybrids, **9**, each with an electron. In the delocalized picture these hybrids combine to form an sp hybrid on carbon pointing away from the hydrogen and a degenerate pair of perpendicular p orbitals, as shown in **10**.

9   **10**

The cobalt fragment has three more electrons than was the case for iron. The MOs for the cobalt cluster do not differ significantly from the iron system, the only change being a shift in the energy ordering of $2a_1$ and $1a_2$. The interaction diagram for $(CO)_9Co_3CH$ is shown in Figure 5.

The 2e set interacts with the set of p orbitals and the $2a_1$ with the carbon lone pair. The $2a_1$ is greatly destabilized and shoots up in energy, and the electrons now occupy the bonding combination of the carbon p's with 2e. $1a_1$ is only slightly raised in energy—we recall here that this MO has a nodal pattern not conducive to bonding above the center.

Using an isolobal analogy[2,12] between the inorganic fragment $Co(CO)_3$ and the organic piece C-H, the system $Co_3(CO)_9CH$ (**11**) has a complement in tetrahedrane C_4H_4 (**12**). The direct correspondence comes out clearly when the

11   **12**
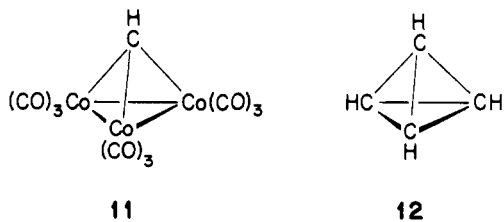
high-lying 2e set is considered and compared to the highest filled π-type orbitals in tetrahedrane, **13** and **14**.

The high-lying filled e set then has p-type symmetry at the apex carbon. A substituent with an acceptor orbital of appro-
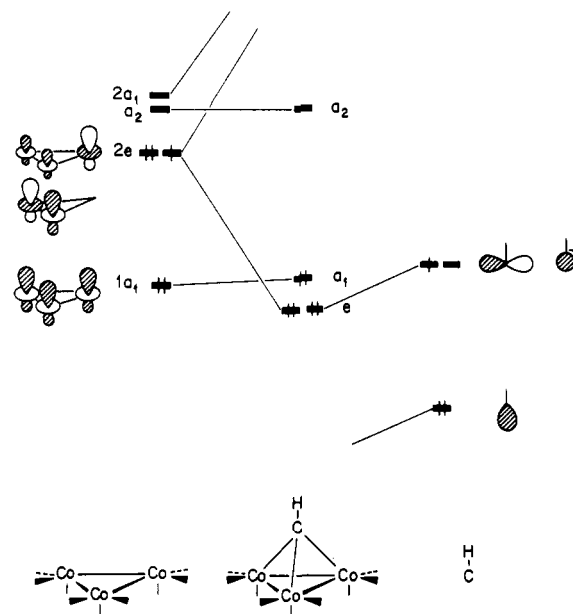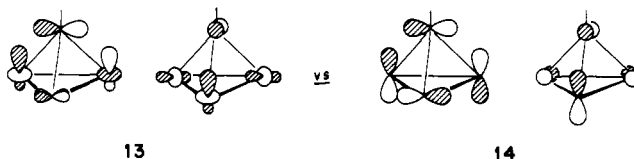

Figure 5. Interaction diagram for $Co_3(CO)_9CH$.

13   **14**

priate symmetry to interact with this e set should be expected to stabilize the complex by withdrawing electron density from the filled MO.[17m] An interesting example of such an acceptor system is encountered in the carbonium ion, **15**. This is the parent molecule of a class widely studied by Seyferth and coworkers.[19]

15
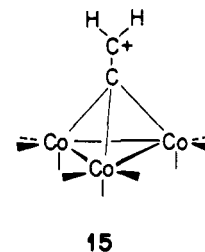
The carbonium ion could also have been constructed by direct use of the $Co_3(CO)_9^+$ fragment, as shown in Figure 6. The reason for this construction will become apparent in a moment. The ligand is then vinylidene C-CH_2. This carbene has two orbitals with p symmetry on the interacting carbon, the high-lying π^*, **16**, and, lower in energy, the carbene p, **17**, both

16   **17**

empty. The donor orbitals, which include the lone pair on carbon, are still lower in energy. **16** and **17** each pick out the appropriate partner from the 2e set, the in-phase combination of **17** then falling below the slightly destabilized $1a_1$. $2a_1$ is greatly destabilized and the system then fills the bonding MO of **17** and one 2e orbital, with the highest filled orbital becoming the destabilized $1a_1$.

The CH_2 group can orient itself in several ways relative to the cluster. Because of the degeneracy of the cluster donor
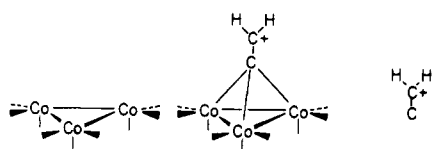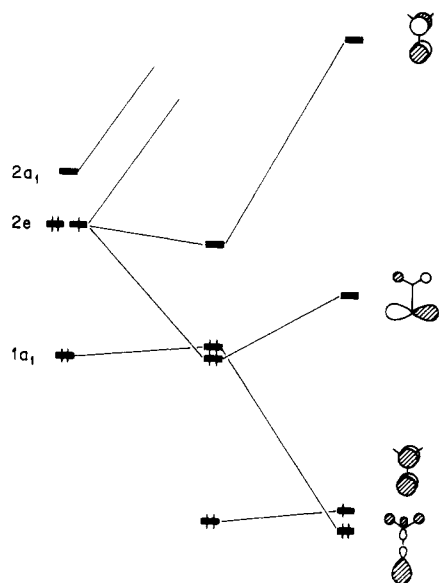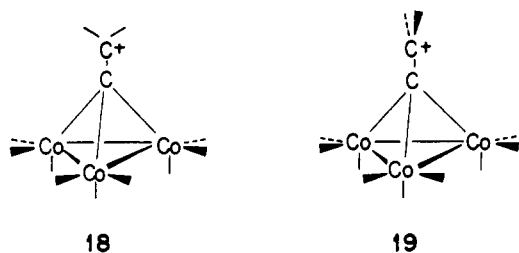
Figure 7. The composite potential energy surface for bending of CCH_2 and CH_2 rotation in the carbonium ion $Co_3(CO)_9CCH_2^+$. The values on the energy contours are in eV.

Figure 6. Diagram showing the interaction of $Co_3(CO)_9^+$ with vinylidene CCH_2.

orbitals the orientation is almost immaterial if the upright position of the C–C bond is maintained. The barrier to rotation between **18** and **19** is sixfold and tiny.

position. There are several degrees of freedom to the deformation. Not only can the CH_2 group bend toward either a metal atom or a metal–metal bond center, but there remains the option of keeping the CH_2 plane perpendicular to the plane of the metals or having the CH_2 group rotated to some degree. The two extremes of this geometrical variation are shown in **22** and **23**.

18   **19**

There remains, however, the possibility that the CCH_2 unit does not stand upright over the center of the ring. One reason to consider this is to be found in the remarkable reaction of ethylene with a refluxing octane solution of the dodecacarbonyls $M_3(CO)_{12}$, $M = Ru$, Os.[20a] Two complexes are formed in each of which the two hydrogens have been stripped from the ethylene, yet retained in the cluster, **20** and **21**. Now

$M_3(CO)_{12}$ $\xrightarrow{C_2H_4}$ **20**   +   **21**

M = Ru,Os   M = Ru
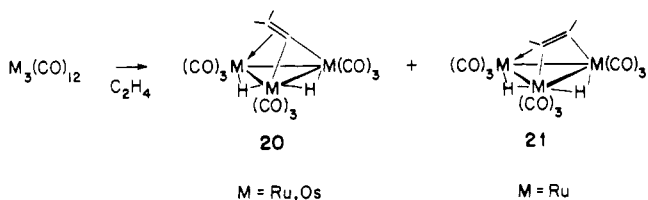
$(CO)_9Co_3CCH_2^+$ is in a sense isoelectronic with **20**, if the two bridging hydrides are counted as protonic. Still closer to the Co cluster is $(CO)_9Os_3H_3CCH_2^+$.[20b] Yet this last molecule, as judged by NMR evidence, and **20**, on the basis of its crystal structure, have the ethylidene σ bonded to two metal atoms, π bonded to the other, in a very unsymmetrical geometry. One should then think about this bonding mode for the cobalt cluster, and this has been suggested by Lewis.

An investigation of this distortion for $(CO)_9Co_3CCH_2^+$ does indeed lead to a preferred conformation away from the upright

22   **23**
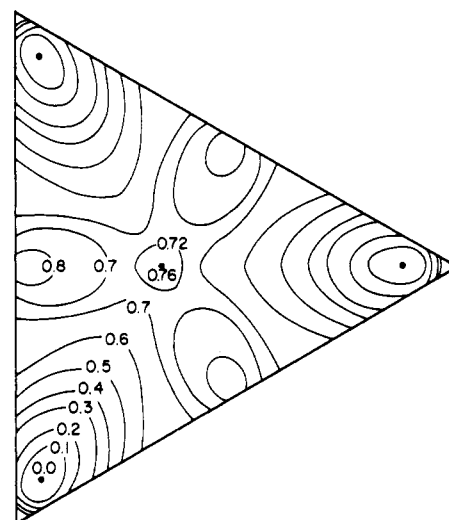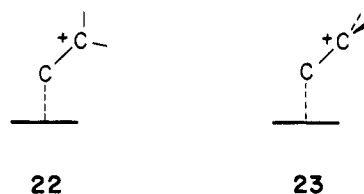
As it turns out, the choice between **22** and **23** is determined by the direction of the bending, **22** being the preferred orientation when CH_2 is moving toward a bond in the metal cluster, whereas the ligand adopts geometry **23** when a metal is approached. The composite potential energy surface, taking into account both deformations, is shown in Figure 7. The circumambulation is accompanied by a CH_2 rotation, as schematically shown in **24**.

24
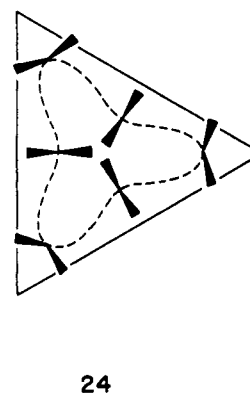
The choice of CH_2 orientation can be understood if we once more regard the highest filled MOs of the cluster, the ones derived from 2e in Figures 5 and 6. When bending toward a metal the symmetric component of 2e is stabilized by increasing overlap between the carbene p orbital and the metal z^2, as shown in **25**. This favorable interaction is not present in the upright position of the hydrogens. However, when ap-
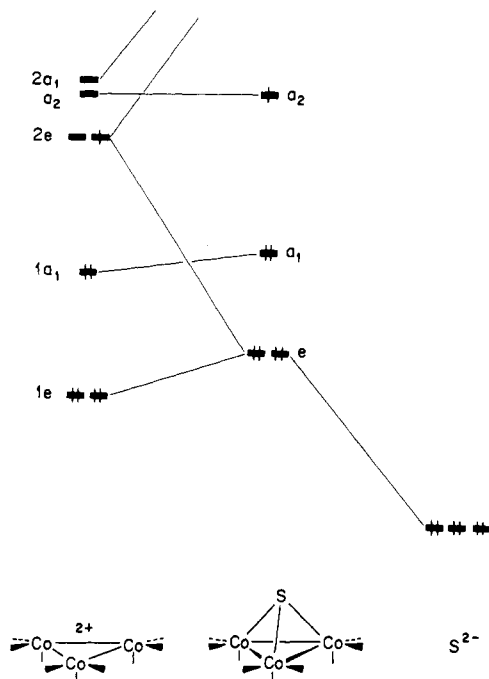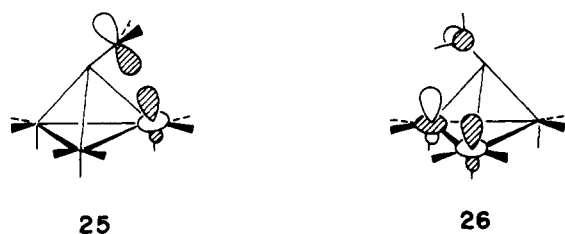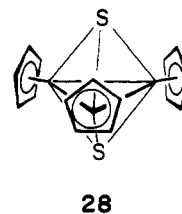
Figure 9. Contour plot of the a_2 orbital in the plane of the three metals. The contours have the values 0.2, 0.1, 0.05, 0.025, and 0.0. The dotted and full lines refer to opposite signs of ψ and the dashed lines are nodal contours.

Figure 8. The orbital interaction diagram for $Co_3(CO)_9{}^{2+}$ and S^{2-}.

proaching a metal–metal bond an interaction with an antisymmetric MO is desired and available, **26**.

25   **26**

The center of the potential surface, the original symmetrical position with no bending, is an energy maximum. This is a consequence of the threefold character of this point, which has three valleys leading away from it. It is a forbidden transition state, in the McIver–Stanton sense,[21] for the interconversion of the distorted structures. Our calculations make the three **26** structures local minima, with **25** as saddle points on the path between structures **26**. The calculated barrier to circumambulation of the ring is 16 kcal/mol. This is somewhat larger than is expected from NMR observations, which indicates a symmetrical or rapidly shifting geometry.[19] However, our study did not include complete geometry optimization. A crystallographic study of one of these molecules would be of great interest, and is underway.[22a] The isolectronic N-iminyl complex $HFe_3(CO)_9(NCHCH_3)$ has a bent structure **25**.[22b]

Note incidentally that the presence of a low-lying empty orbital in the upright structure of Figure 6 might have led one to expect a deformation, on the basis of a second-order Jahn–Teller argument.

We now turn to the sulfur atom or another chalcogenide, **27**,

27

as a capping ligand, then to two sulfur atoms, and to one or two carbonyl group.

The low-lying p orbitals on sulfur are filled, when we for-

mally consider sulfur as doubly negative, interacting with a cobalt fragment, $Co_3(CO)_9{}^{2+}$, as shown in Figure 8. The 2e set, together with the lower 1e, interacts strongly with these p's. The $1a_1$ is slightly destabilized by the p_z on sulfur, whereas $2a_1$ is pushed out of reach. The a_2 orbital does not interact at all and stays fairly low in energy.

When adding in electrons, let us first consider the positively charged cluster, $Co_3(CO)_9S^+$. Here the orbitals are filled through the $1a_1$. The extra electron needed to produce the neutral $Co_3(CO)_9S$ will then go into the metal–metal antibonding orbital a_2, a plot of which is shown in Figure 9. This has already been suggested by Dahl and co-workers.[23] As a result one would expect a weakening of the Co–Co bond. The overlap population between the cobalts is indeed reduced by more than a factor of 2. This result is in perfect accordance with the structural data found for the systems $Co_3(CO)_9S$ and $Co_2Fe(CO)_9S$, the latter isoelectronic with $Co_3(CO)_9S^+$.[23] The distance between the cobalt atoms increases by nearly 0.10 Å in going from the mixed cluster to the system with one more electron.

If we now recall the C–H system discussed earlier, $Co_3(CO)_9CH$, the lowest empty orbital in that cobalt cluster is again the a_2 orbital and an additional electron should occupy this MO. An example would here be the paramagnetic $Ni_3Cp_3(NR)$ cluster,[24] isoelectronic with $Co_3(CO)_9CR^-$. ESR studies on $Co_3(CO)_9CY^-$ clusters confirm that the singly occupied orbital is of a_2 symmetry.[25] Photochemical studies of $Co_3(CO)_9CY$ compounds lead to a breakup of the cluster, which seems in accord with the metal–metal antibonding character of the empty MO.[26]

A very similar picture emerges when the disulfur system is considered. Here the sulfur atoms are attached to both sides of the cluster, **28**, a configuration observed for other ligands

28

as well, with the terminal groups either carbonyls or cyclopentadienyl rings. We shall discuss here only the clusters where the additional ligands are sulfur or carbonyl, but structures with other groups are known.[27]
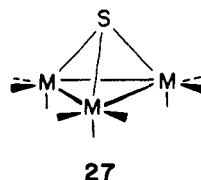
A steady diminution in bond length when going down the series $Co_3Cp_3S_2$, $Co_3Cp_3S_2^+$, and $Co_3Cp_3(S)(CO)$[28] makes one wonder which orbital the electrons are coming from—once again the a_2 orbital has been suggested.[28]

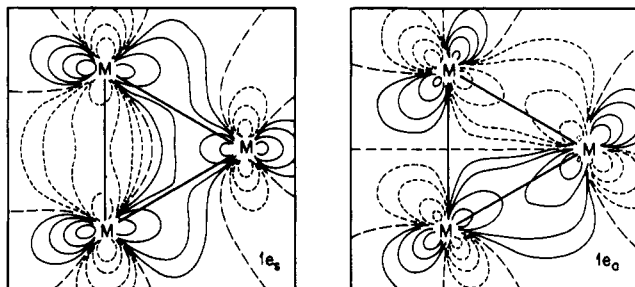The fragment appropriate in this context has three cyclo-

Figure 10. Plots of the 1e orbitals shown in the plane containing the metal triangle. Contour values are 0.2, 0.1, 0.05, 0.025, and 0.0. Dotted lines refer to negative contours; dashed lines are nodes.

pentadienyl groups substituted for the terminal carbonyls, but the change in fragment orbitals is very small. The only observable difference is a tilting of the 2e, such that it has more xz/yz character on the metal. This provides for overlap with ligands on both sides of the base.

Before we discuss the dicarbonyl system[29] we will briefly go through the bonding of a single carbonyl approaching along the threefold axis, **29**. The interaction is simple; the 2e gets

29   **30**
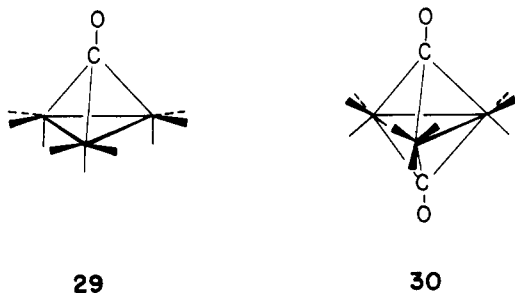
stabilized by the π^*, and the donor orbital interacts in a typical three-orbital manner with a lower lying cluster orbital and $2a_1$, where the latter MO prevents the interaction with the filled orbital from becoming too pronounced. When two carbonyls are introduced, **30**, the picture is very similar, the highest occupied MO being the stabilized 2e. For $Co_3Cp_3(CO)_2$ this degenerate set would be half occupied.

If two sulfurs are bonded to the cluster, the e sets are destabilized by the π donors just as in the monosulfur system. In this case the two additional electrons do, however, go into the a_2 orbital. This MO does not take part in bonding and is thus still low lying and available. The intermediate system, $Co_3Cp_3(CO)(S)$, has one e set stabilized by the carbonyl π^*, but the level ordering remains the same, and the a_2 is now the lowest empty orbital. When comparing the three systems, the disulfur compound does indeed have two electrons in a metal–metal antibonding MO and is therefore expected to have the longest bond, the monopositive disulfur system one electron in a_2, so a somewhat shorter bond, and the carbonyl–sulfur cluster the shortest bond, with no electrons in a_2. The reader is referred to the papers of Dahl and co-workers for a detailed discussion of the structural and electronic characteristics of these molecules.[28]

Acyclic Unsaturated Ligands

Olefins react with both ruthenium and osmium clusters to give a range of trinuclear products. The bonding of ethylene occurs with transfer of two hydrogens to the cluster,[20,30] leaving the carbon system bonded in one of two ways shown previously, as a vinylidene, **20**, or an acetylene, **21**. Here we will discuss the bonding of C_2H_4 and C_2H_2 in relation to those structures, with more detailed discussion of the acetylene cluster.
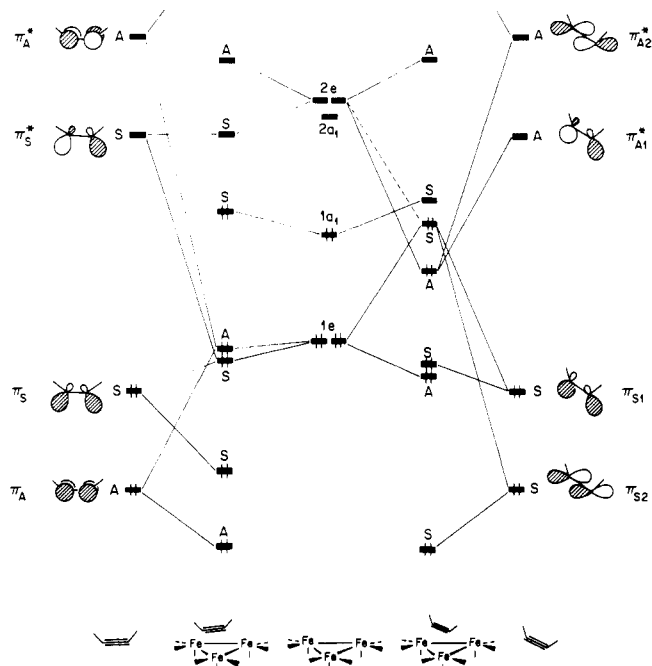

Figure 11. Interaction diagram for $Fe_3(CO)_9$ and acetylene in the two conformations discussed in the text. The perpendicular conformation is at the left in the diagram, the parallel to the right.

In the clusters with unsaturated ligands the atoms of the ligand are no longer centered over the cluster midpoint. This, together with a shorter distance to the metal plane, gives more involvement of the 1e set in the bonding. Plots of these orbitals, the bonding combinations of the local xy of the metal, are shown in Figure 10 for future reference.

In our calculations of the C_2H_4 cluster, the ethylene is not bound. Two possible orientations of the olefin are shown in **31** and **32**. Both suffer from unfavorable interactions with filled ethylene orbitals, in particular **33** and **34**. The $1a_1$ and $1e_s$ of

31   **32**

33   **34**
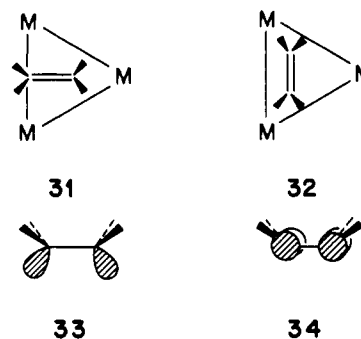
the M_3L_9 fragment are destabilized by **33**, $1e_a$ by **34**. The ethylene π^* enters to ameliorate one of these four-electron repulsions, but it does nothing for the other. It has been suggested by a referee that if the ethylene were shifted over to lie above a single metal atom binding would occur. This is certainly possible, but has not as yet been investigated by us.

The disadvantage of having a π^* of only a single symmetry is no longer necessarily present in the acetylene system. Depending on the orientation, **35** or **36**, the empty π^* are of opposite symmetries (see **37**) or of the same symmetry (**38**).

The interaction diagram for the two orientations is shown in Figure 11. The cluster orbitals mainly involved in the interaction are the 1e and 2e sets. $1a_1$ is only slightly affected in both conformations.

As expected in view of the previous argument, **35** is most stable. Here both symmetric and antisymmetric ligand orbitals are present in the filled and empty manifold. The interaction
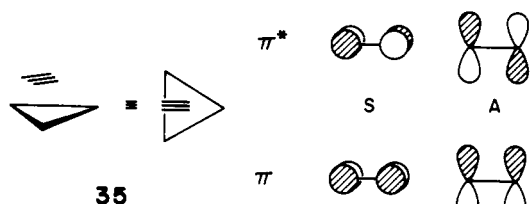
35
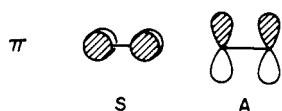
37
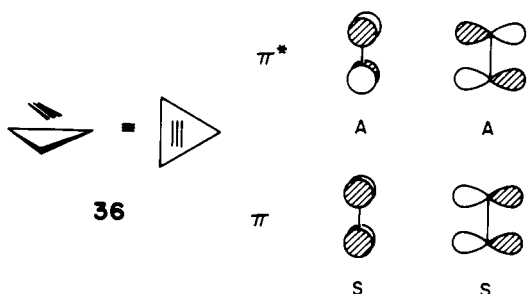
36

38

between the symmetric $1e_s$ and the acetylene π_S and π_S^* exhibit a familiar three-orbital mixing pattern with the middle orbital, $1e_s$, changing only slightly in energy. Some stabilization by $2e_s$ is observed for the highest MO.

The antisymmetric orbitals display a similar behavior; again $1e_a$ changes only a little in energy. The overall effect on the filled cluster orbitals is thus small.

We now turn to the other orientation, **36**, where both π orbitals are symmetric and both π^*'s antisymmetric. Again the symmetric orbitals $1e_s$, π_{S1}, and π_{S2} comprise a set of three interacting MOs but here they are all filled and the net effect is destabilizing.

The π^* orbitals interact with the cluster MO $2e_a$ in a similar fashion. However, here the interaction is between empty orbitals and the net stabilization arises only because the lowest of the antisymmetric MOs falls below the filled symmetric orbitals. The energy gain is small. $1e_a$ is lowered only slightly by the energetically distant π^*'s. Thus the dominant feature in **36** is destabilization by the filled π orbitals, causing this conformation to be the less stable.

Good binding of an olefin to a cluster is thus dependent on the presence of filled and unfilled orbitals of similar symmetry. The alternative ethylidene structure, **20**, has two such orbitals. These were illustrated earlier, **16** and **17**, in the context of the discussion of $Co_3(CO)_9CCH_2^+$.

The acetylene cluster, $H_2Ru_3(CO)_9(C_2H_2)$, **21**, has the acetylene parallel to a metal–metal bond. If we again count the hydrogens as protonic, this cluster is isoelectronic with $Fe_3(CO)_9(C_2H_2)^{2-}$. Adding two elelctrons to the iron–acetylene cluster discussed so far, we see that they go into highest symmetric MO in Figure 11. In the perpendicular conformation this is the destabilized symmetric π^*_S, high in energy. In **36**, however, we fill the slightly destabilized $1a_1$, empty due to the appearance of an antisymmetric MO, the result of the stabilizing interaction between the π^* orbitals and $2e_a$. Thus, as before we suffered the unfavorable consequences of the destabilization by symmetric π orbitals, we now reap the full benefits of the stabilization between the antisymmetric MOs. One way of describing this is that the interaction no longer is between empty orbitals, but rather a filled orbital is stabilized by an empty orbital on the other fragment. In the perpendicular system this filled fragment MO is destabilized. As a consequence, the low-energy conformation is no longer **35**, but has

the acetylene parallel to a metal–metal bond, **36**. The observed geometries of the two types of clusters may also be explained in terms of the polyhedral skeletal electron pair theory.[1e]

A crystal structure of a neutral acetylene iron cluster has the olefin in the predicted orientation, **35**,[5,31] but displaced toward the metal–metal bond, **39**. An analysis of this distortion
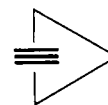
39

does indeed give a calculated minimum when the olefin moves in that direction; specifically, an optimum displacement of the bond center 0.27 Å from a position directly above the cluster center is computed. The orbitals primarily responsible for this energy variation are the A and S orbitals derived from $1e$.[32a]

The presence of three equivalent acetylene orientations of type **35** or **36** raises the question of how the molecules move between these minima. We have analyzed this problem, and propose elsewhere a series of intricate rearrangement pathways.[32b]

Proceeding to larger systems we will first analyze the C_3H_3 ligand, both in its open and, in the following section, in its closed form. The open structure is found in several ruthenium compounds with the conformation **40**, where the ligand is bound in an allylic fashion to one metal, but is thought to have σ bonds to the two remaining metals.[33]

40   **41**

Calculations of the open C_3H_3 system do indeed give **40** as the most stable form, with **41** a maximum along the potential energy profile for rotation. The main stabilization comes from the interaction of the nonbonding π orbital, **42**, on the C_3H_3. This favorable interplay, mainly with the $1e$ on the cluster, leads to bond formation with the two symmetrically disposed metals, stronger in character than with the unique metal atom, as is apparent from the overlap populations quoted below.
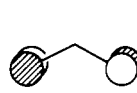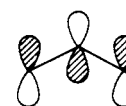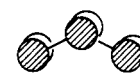
42   **43**   **44**

45

The interaction with the nonbonding MO itself is, however, the same in the two orientations since the center carbon has only been "flipped" over. The barrier to rotation thus must have another origin. The C_3H_3 system has two symmetric orbitals fairly low in energy. One, **44**, is the π orbital, and **43**, a σ orbital or radical lobe combination. These lie just below **42** in energy. In orientation **40** the π combines out of phase with $1e_s$ and $1a_1$ and **43** mixes into this in a bonding manner. When the orientation is reversed the bonding interaction between the central carbon and the unique metal is lost and the orbital is greatly destabilized.

The actual crystal structures have an additional hydrogen bonded to the system. Speculations have been made as to where the hydride is attached, using the elongation of the unique metal–metal bond as an indication of a bridged atom. Attack of a hydride on the metal base of the monopositive system given a calculated preference for the hydrogen in the metal plane doubly bridging the metals. The symmetric position underneath the cluster is definitely unfavorable.

Donation of electrons from the nonbonding MO, **42,** into an orbital antisymmetric with respect to the vertical mirror plane should tend to weaken the M–M bond straddling that plane. The calculated overlap populations do indicate a decrease in bond strength, which should lead to a lengthening of the metal–metal bond. This indeed happens in $Ru_3(CO)_9$-(C_6H_{10}),[33a] where the unique Ru–Ru distance is 2.96 Å, while the others are 2.78 Å. The conclusion of this kind of analysis, that the longer unique metal–metal bond is a result of the bonding of the allyl fragment and less so because of the bridging hydrogen, is substantiated by considering other hydrogen-bridged complexes. In $HFe_3(CO)_9(S$-i-$C_3H_7)$[17j] the hydrogen is definitely doubly bridging, being 1.0 Å below the plane, copolanar with the sulfur and two irons. In the complex $HRu_3(CO)_{10}(C=NMe_2)$[17i] the hydrogen-bridged bond is actually shortened with respect to the other bonds, 2.80 and 2.83, 2.83 Å, respectively. In complexes of this kind with triply bridging groups the geometry might be mainly determined by the bonding pattern of these larger groups while the hydrogen has less influence on the structure.

In $Ru_3(CO)_9(C_{12}H_{15})$[33b] three carbons are equally distant from one ruthenium whereas two other carbon atoms appear to be σ bonded to a metal such that the ring system is bonded in an allylic fashion. In accordance with this pattern one metal bond is longer, 2.92 Å compared to 2.77 and 2.77 Å for the other two.

Clusters with polyene ligands containing one or two more carbons, butadiene and the pentadienyl system, respectively, are computed to have **46** and **47** as their most stable confor-

46   **47**
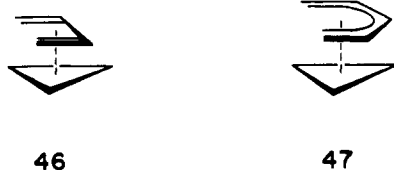
mations. No structures of butadiene complexes bonded in this fashion are known, and the calculations do indicate a lack of stabilization. This is mainly due to a repulsive interaction of the HOMO, **48,** with $1e_a$.


48   **49**   **50**
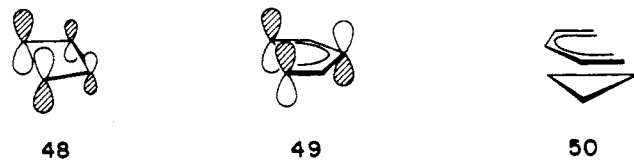
The crystal structure of $HOs_3(CO)_9C_6H_7$ has the six-membered ring bonded through five carbons in a pentadienyl fashion.[34] The pentadienyl has a low-lying nonbonding symmetric orbital, **49,** which in the conformation **47** almost coincides with the $2e_s$ of the cluster. This favorable interaction is lost and the interaction with $1e$ turned on when the ligand is rotated to conformation **50.** The nodal pattern of $1e_s$, as Figure 10 shows, is such that the lobes of **49** lie close to nodes in conformation **47** but fall in the bonding regions in **50.** The molecule in the crystal does indeed adopt conformation **47.**

Cyclic Unsaturated Ligands

The closed three-membered carbon ring fits perfectly on top of the triangular metal face, **51,** though the geometric con-

gruence need not imply good overlap. In fact there is a nice match between the ligand π^* set, of e symmetry, and M_3L_9 2e. Unfortunately there is also a strong destabilizing interaction between filled orbitals—a ligand Walsh orbital set and M_3L_9 1e. In our calculations **51** is not bound; the stable complex has the ring rotated by 60°, **52.** In this orientation the overlap is

51   **52**
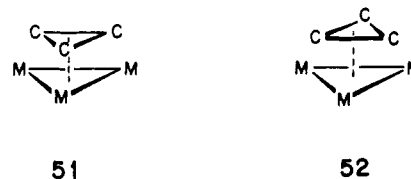
much poorer and both interactions between the four e sets are reduced. The destabilization of 1e is avoided.

A complex with a cyclopentadienyl π bonded to the face of a rhodium cluster, $(\pi$-$Cp)_4Rh_3H$, has been structurally characterized as **3,** schematically shown in **53.** The Rh_3Cp_3

53

cluster is isoelectronic with our model system $Fe_3(CO)_9$, so calculations were carried out using the latter. The singly noded e'_1 set of the Cp ring is filled, and when interacting with the 1e gives a four-orbital eight-electron destabilization. The destabilized $1a_1$ is filled in the mononegative system, where we take into account the presence of an additional hydrogen. The stabilization of the system is due to the lower lying filled orbitals. The nature of the e orbitals on the organic ligand is such that no orientational preference is observed.

A very similar picture emerges when benzene is considered. The overlap of the benzene π systems with the cluster is somewhat better, but the filled degenerate set is lower in energy, destabilizing 1e somewhat less. For the neutral iron system, the benzene acting as a six-electron donor, the levels are filled through the destabilized $1a_1$ and the net effect is destabilizing. A stabilization can only be obtained when the overlap of the lower filled e set, the benzene donor orbitals, with the filled 1e is poor, maximizing the stabilizing effect of the π^* of benzene as well as enjoying the donor–acceptor interaction of the filled π's and 2e.

For two less electrons the system is more stable when the $1a_1$ is no longer filled. However, the structural evidence at hand does not suggest this conformation. The $HOs_3(CO)_9C_6H_7$ cluster mentioned above does not adopt conformation **54** but rather the isomeric **55,** where the ligand is attached through five carbons.

54   **55**
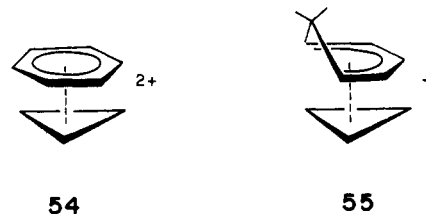
An ML₂ Cap

An interesting product of the reaction of $Pt(C_2H_4)_2PR_3$ with the dihydrido complex $H_2Os_3(CO)_{10}$ is the PtLL′ capped cluster $Os_3Pt(\mu$-$H)_2(CO)_{10}PR_3$.[35] Bridging hydrogens between Os–Pt and along one Os–Os edge are suspected. If we ignore for a moment the problem of the hydride locations, and treat these ligands as protons, we come to a hypothetical $Os_3(CO)_9PtL_2^{2-}$, **56.**

Table I. Parameters Used in Extended Hückel Calculations

orbital	H_{ii}, eV	ζ_1	ζ_2	$c_1{}^a$	$c_2{}^a$
Fe 3d	−12.70	5.35	1.80	0.5366	0.6678
4s	−9.17	1.90			
4p	−5.37	1.90			
Co 3d	−13.18	5.55	2.10	0.5679	0.6059
4s	−9.21	2.00			
4p	−5.29	2.00			
Pt 5d	−13.43	6.013	2.696	0.6334	0.5513
6s	−9.57	2.554			
6p	−5.86	2.554			
C 2s	−21.40	1.625			
2p	−11.40	1.625			
O 2s	−32.30	2.275			
2p	−14.80	2.275			
P 3s	−18.60	1.60			
3p	−14.00	1.60			
S 3s	−20.0	1.817			
3p	−13.3	1.817			
H 1s	−13.60	1.30			

^{a} Contraction coefficients used in the double ζ expansion.

56

Figure 12. Orbital interaction diagram of $Fe_3(CO)_9{}^{2-}$ and $Pt(CO)_2$. The symmetry labels on the MOs of the platinum fragment refer to the C_{2v} symmetry of $Pt(CO)_2$.

As a prototype for this type of molecule we chose to analyze the system with a capping $Pt(CO)_2$ group. An interaction diagram for this molecule is constructed in Figure 12 from the well-known orbitals of an ML_2 fragment,[36] and the now familiar M_3L_9 orbitals. Only the HOMO of the $Pt(CO)_2$ fragment is shown. Lower in energy lie the four orbitals that together with the b_2 make up the five metal d orbitals. The b_2 picks out one component of the 2e set leading to a stabilizing interaction. The other partner of the 2e set finds a match in a low-lying empty b_1 orbital. The other major energy gain is obtained through an interaction between the cluster $2a_1$, concentrated above the metal base and filled in the doubly negative system, and a low-lying empty hybrid orbital on the platinum. This orbital is a mixture of z^2 and p_z and is hybridized toward the cluster with excellent overlap with $2a_1$. We observe from the diagram the presence of low-lying empty orbitals, in accord with the color and unsaturation of the cluster.

The barrier to rotation of the platinum fragment above the cluster is tiny. This is to be expected as the two main interactions involve one of a_1 symmetry, invariant under rotation, and a 2e set on the cluster, where the b_2 of the ML_2 ligand picks the appropriate partner to bond to.

A similar picture emerges when the unsymmetrical capping ligand $Pt(CO)(PH_3)$, is considered. Again the barrier to rotation is small, 6 kcal/mol, with the calculated minimum conformation, **57**, and the 30° rotated structure **59** a maximum on the energy profile. The other symmetric isomer, **58**, is close in energy to **57**. The sl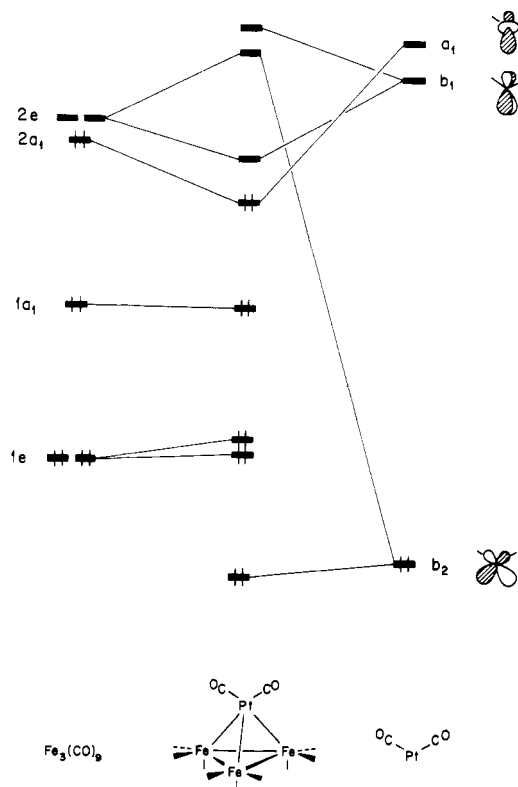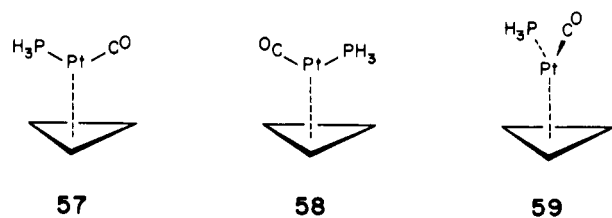ightly larger barrier to rotation finds its origin in the changed character of the ML_2 fragment MOs. The reduction of symmetry from C_{2v} to C_s produces a tilting of the orbitals, which results in enhanced overlap in structures **57** and **58** with the cluster MOs. The structural evidence does seem to point toward a conformation like **58** rather than **59**. The bulk of the phosphine ligand as well as the asymmetry introduced by the hydrides will play a role in determining the actual geometry.

One interesting structural alternative for these PtL_2 capped clusters, suggested to us by T. A. Albright, is a slipping of the PtL_2 toward a M–M bond, with the PtL_2 plane parallel to a M–M bond. Such slipping distortions are found in carbametallaboranes,[37a] and have been suggested for other organometallic complexes as well.[37b] From the published structural information this does not seem to happen in the case examined so far, but should be kept in mind as further structures of this type are synthesized.

Concluding Remarks

Perhaps it is appropriate to end on a note of humility. We feel that through this study of one subclass of trinuclear clusters we have begun to understand the geometrical and electronic features of this important group of transition metal compounds. But there is no chance that a theoretical analysis of this kind can stay ahead of the wondrous and awesome complexity of molecules which are continuously revealed to us. Let **60**,[32c] **61**,[38a] and **62**[38b] stand as examples, not to speak of the intricate mechanism that led to these lovely structures.
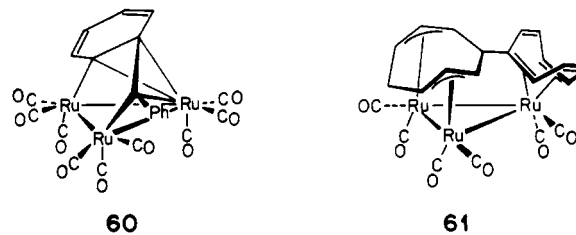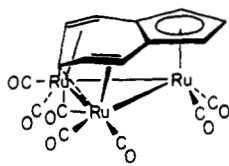
57   **58**   **59**

60   **61**

62

Appendix

The orbital exponents and H_{ii}'s for the extended Hückel calculations[39] were obtained from earlier work[3c,16c] and are listed in Table I. The basic geometry of the cluster systems consisted of an equilateral triangle of metals with metal–metal separations of 2.64 and 2.47 Å for Fe and Co, respectively. Terminally bonded to each metal with bond lengths of 1.86 (Fe–C) and 1.80 Å (Co–C) were one axial and two equatorial carbonyls, the latter separated by an angle of 115°. The capping ligands were placed 1.5 Å above the metal base for the singly bonded ligands, 1.37 Å for acetylene and ethylene, and 2.0 Å for four- and five-membered acyclic olefins and the cyclic π systems. The center atoms of the open C_3H_3 was tilted an angle of 41° away from the metal plane keeping a distance of 2.0 Å. The C–C bond lengths were 1.53 (CCH_2), 1.29 (C_2H_2), 1.37 (C_2H_4), and 1.36 Å (C_3H_3), and 1.41 Å in all larger membered systems. All C–H bonds were set at 1.09 Å. The Pt–C(O) distance was 1.86 Å, the angle between the carbonyls 140°, and the distance to the metal plane 2.31 Å.

References and Notes

(1) (a) Review of clusters in general: R. B. King, *Prog. Inorg. Chem.*, **15**, 287 (1972). (b) Review of Ru and Os clusters: S. C. Tripathi, S. C. Srivastava, R. P. Mani, and A. K. Shrimal, *Inorg. Chim. Acta*, **15**, 249 (1975). (c) Review of clusters with π-acid ligands: R. D. Johnston, *Adv. Inorg. Chem. Radiochem.*, **13**, 471 (1970). (d) Review of cobalt clusters: B. R. Penfold and B. H. Robinson, *Acc. Chem. Res.*, **6**, 73 (1973); G. Pályi, F. Piacenti, and L. Markó, *Inorg. Chim. Acta Rev.*, **4**, 109 (1970); G. Schmid, *Angew. Chem.*, **90**, 417 (1978). (e) D. M. P. Mingos, *Adv. Organomet. Chem.*, **15**, 1 (1977); R. Mason and D. M. P. Mingos, *MTP Int. Rev. Sci.: Phys. Sci., Ser. Two*, **11**, 121 (1975).
(2) For general theories of cluster bonding see (a) K. Wade, "Electron Deficient Compounds", Nelson, London, 1971; *Adv. Inorg. Chem. Radiochem.*, **18**, 1 (1976); (b) D. M. P. Mingos, *Nature (London), Phys. Sci.*, **236**, 99 (1972); (c) J. W. Lauher, *J. Am. Chem. Soc.*, **100**, 5305 (1978).
(3) (a) P. J. Hay, J. C. Thibeault, and R. Hoffmann, *J. Am. Chem. Soc.*, **97**, 4884 (1975); (b) J. W. Lauher, M. Elian, R. H. Summerville, and R. Hoffmann, *ibid.*, **98**, 3219 (1976); (c) R. H. Summerville and R. Hoffmann, *ibid.*, **98**, 7240 (1976); (d) D. L. Thorn and R. Hoffmann, *Inorg. Chem.*, **17**, 126 (1978); (e) A. Dedieu and R. Hoffmann, *J. Am. Chem. Soc.*, **100**, 2074 (1978).
(4) P. W. Sutton and L. F. Dahl, *J. Am. Chem. Soc.*, **89**, 261 (1967).
(5) J. F. Blount, L. F. Dahl, C. Hoogzand, and W. Hübel, *J. Am. Chem. Soc.*, **88**, 292 (1966); W. Hubel and E. H. Braye, *J. Inorg. Nucl. Chem.*, **10**, 250 (1959).
(6) E. O. Fischer, O. S. Mills, E. F. Paulus, and H. Waversik, *Chem. Commun.*, 643 (1967).
(7) E. R. Corey and L. F. Dahl, *J. Am. Chem. Soc.*, **83**, 2203 (1961); *Inorg. Chem.*, **1**, 521 (1962); R. Mason and A. I. M. Rae, *J. Chem. Soc. A*, 778 (1968); M. R. Churchill and B. G. DeBoer, *Inorg. Chem.*, **16**, 878 (1977); M. R. Churchill, F. J. Hollander, and J. P. Hutchinson, *ibid.*, **16**, 2655 (1977). A diarsenic substituted Ru cluster; P. J. Roberts and J. Trotter, *J. Chem. Soc. A*, 1479 (1971). Hydride and phosphine substituted Os clusters; M. R. Churchill and B. G. DeBoer, *Inorg. Chem.*, **16**, 2397 (1977); C. W. Bradford, R. S. Nyholm, G. J. Gainsford, J. M. Guss, P. R. Ireland, and R. Mason, *J. Chem. Soc., Chem. Commun.*, 87 (1972). The structurally similar Mn–hydride cluster, $Mn_3(CO)_{12}H_3$: S. W. Kirtley, J. P. Olsen, and R. Bau, *J. Am. Chem. Soc.*, **95**, 4532 (1973).
(8) C. H. Wei and L. F. Dahl, *J. Am. Chem. Soc.*, **91**, 1351 (1969); F. A. Cotton and J. M. Troup, *ibid.*, **96**, 4155 (1974). A diphosphine substituted cluster; G. Raper and W. S. McDonald, *J. Chem. Soc. A*, 3430 (1971).
(9) (a) F. A. Cotton and D. L. Hunter, *Inorg. Chim. Acta*, **11**, I9 (1974); F. A. Cotton, B. E. Hanson, and J. D. Jamerson, *J. Am. Chem. Soc.*, **99**, 6588 (1977); (b) O. A. Gansow, A. R. Burke, and W. D. Vernon, *ibid.*, **94**, 2550 (1972); (c) J. Evans, B. F. G. Johnson, J. Lewis, and T. W. Matheson, *J. Organomet. Chem.*, **97**, C16 (1975); A. Forster, B. F. G. Johnson, J. Lewis,

T. W. Matheson, B. H. Robinson, and W. G. Jackson, *J. Chem. Soc., Chem. Commun.* 1042 (1974); E. G. Bryan, B. F. G. Johnson, and J. Lewis, *J. Chem. Soc., Dalton Trans.*, 144 (1977); (d) S. Aime, O. Gambino, L. Milone, E. Sappa, and E. Rosenberg, *Inorg. Chim. Acta*, **15**, 53 (1975); S. Aime, L. Milone, D. Osella, M. Valle, and E. W. Randall, *ibid.*, **20**, 217 (1976); L. Milone, S. Aime, E. W. Randall, and E. Rosenberg, *J. Chem. Soc., Chem. Commun.*, 452 (1975); (e) J. R. Shapley, S. I. Richter, M. Tachikawa, and J. B. Keister, *J. Organomet. Chem.*, **94**, C43 (1975); (f) B. F. G. Johnson, *J. Chem. Soc., Chem. Commun.*, 211, 703 (1976).
(10) (a) M. Elian and R. Hoffmann, *Inorg. Chem.*, **14**, 1058 (1975); (b) J. K. Burdett, *J. Chem. Soc., Faraday Trans. 2*, **70**, 1599 (1974); *Inorg. Chem.*, **14**, 375 (1975).
(11) (a) J. F. Harrison, *Acc. Chem. Res.*, **7**, 378 (1974); (b) R. Hoffmann, G. D. Zeiss, and G. W. Van Dine, *J. Am. Chem. Soc.*, **90**, 1485 (1968).
(12) M. Elian, M. M.-L. Chen, D. M. P. Mingos, and R. Hoffmann, *Inorg. Chem.*, **15**, 1148 (1976); ref 2.
(13) (a) W. L. Jorgensen and L. Salem, "The Organic Chemist's Book of Orbitals", Academic Press, New York, 1973; (b) R. Hoffmann, "Special Lectures at XXIIIrd International Congress of Pure and Applied Chemistry", Vol. 1, Butterworths, London, 1971, p 157.
(14) (a) D. V. Korol'kov and H. Miessner, *Z. Phys. Chem. (Leipzig)*, **253**, 25 (1973); (b) D. R. Tyler, R. A. Leverson, and H. B. Gray, *J. Am. Chem. Soc.*, **100**, 7888 (1978).
(15) J. C. Green, private communication.
(16) (a) L. E. Orgel, *J. Inorg. Nucl. Chem.*, **2**, 315 (1956); (b) S. F. A. Kettle, *Inorg. Chem.*, **4**, 1661 (1965); (c) T. M. Whitesides, D. L. Lichtenberger, and R. A. Budnik, *ibid.*, **14**, 68 (1975); (d) D. L. Lichtenberger and R. F. Fenske, *J. Am. Chem. Soc.*, **98**, 50 (1976); (e) T. A. Albright, P. Hofmann, and R. Hoffmann, *ibid.*, **99**, 7546 (1977).
(17) (a) J. P. Yesinowski and D. Bailey, *J. Organomet. Chem.*, **65**, C27 (1974); (b) G. M. Sheldrik and J. P. Yesinowski, *J. Chem. Soc., Dalton Trans.*, 873 (1975); (c) R. J. Dellaca and B. R. Penfold, *Inorg. Chem.*, **11**, 1855 (1972); (d) M. R. Churchill, B. G. DeBoer, and F. J. Rotella, *Inorg. Chem.*, **15**, 1843 (1976); (e) V. Batzel, U. Müller, and R. Allmann, *J. Organomet. Chem.*, **102**, 109 (1975); V. Batzel, *Z. Naturforsch. B*, **31**, 342 (1976); G. Schmid and V. Bätzel, *J. Organomet. Chem.*, **46**, 149 (1972); (f) V. Batzel and G. Schmid, *Chem. Ber.*, **109**, 3339 (1976); (g) G. Schmid, V. Batzel, and B. Stutte, *J. Organomet. Chem.*, **113**, 67 (1976); (h) M. D. Brice, R. J. Dellaca, B. R. Penfold, and J. L. Spencer, *Chem. Commun.*, 72 (1971); (i) M. R. Churchill, B. G. DeBoer, F. J. Rotella, E. W. Able, and R. J. Rowley, *J. Am. Chem. Soc.*, **97**, 7158 (1975); (j) R. Bau, B. Don, R. Greatrex, R. J. Haines, R. A. Love, and R. D. Wilson, *Inorg. Chem.*, **14**, 3021 (1975); (k) F. Klanberg, W. B. Askew, and L. J. Guggenberger, *Inorg. Chem.*, **7**, 2265 (1968); (l) G. Schmid and G. Etzroth, *J. Organomet. Chem.*, **137**, 367 (1977). (m) For a discussion of the transmission of electronic effects in these clusters see D. C. Miller and T. B. Brill, *Inorg. Chem.*, **17**, 240 (1978). (n) G. Schmid, B. Stutte, and B. Roland, *Chem. Ber.*, **111**, 1239 (1978); B. Stutte, V. Batzel, R. Boese, and G. Schmid, *ibid.*, **111**, 1603 (1978).
(18) (a) R. J. Dellaca, B. R. Penfold, B. H. Robinson, W. T. Robinson, and J. L. Spencer, *Inorg. Chem.*, **9**, 2197 (1970); (b) M. D. Brice and B. R. Penfold, *ibid.*, **11**, 1381 (1972); (c) D. Seyferth, R. J. Spohn, M. R. Churchill, K. Gold, and F. R. Scholer, *J. Organomet. Chem.*, **23**, 237 (1970); (d) R. J. Dellaca and B. R. Penfold, *Inorg. Chem.*, **10**, 1269 (1971); (e) G. Allegra, E. M. Peronaci, and R. Ercoli, *Chem. Commun.*, 549 (1966); (f) G. Allegra and S. Valle, *Acta Crystallogr., Sect. B*, **25**, 107 (1969).
(19) D. Seyferth, G. H. Williams, and J. E. Hallgren, *J. Am. Chem. Soc.*, **95**, 266 (1973); D. Seyferth, G. H. Williams, and D. D. Traficante, *ibid.*, **96**, 604 (1974). For a review see D. Seyferth, *Adv. Organomet. Chem.*, **14**, 97 (1976).
(20) (a) A. J. Deeming and M. Underhill, *J. Chem. Soc., Dalton Trans.*, 1415 (1974); *J. Organomet. Chem.*, **42**, C60 (1972); *J. Chem. Soc., Chem. Commun.*, 277 (1973); (b) A. J. Deeming, S. Hasso, M. Underhill, A. J. Canty, B. F. G. Johnson, W. G. Jackson, J. Lewis, and T. W. Matheson, *J. Chem. Soc., Chem. Commun.*, 807 (1974).
(21) R. E. Stanton and J. W. McIver, Jr., *J. Am. Chem. Soc.*, **97**, 3632 (1975); J. N. Murrell and K. J. Laidler, *Trans. Faraday Soc.*, **64**, 371 (1968).
(22) (a) B. H. Robinson, personal communication; (b) M. A. Andrews and H. D. Kaesz, *J. Am. Chem. Soc.*, **99**, 6763 (1977); M. A. Andrews, B. v. Buskirk, C. B. Knobler, and H. D. Kaesz, to be published.
(23) (a) C. E. Strouse and L. F. Dahl, *Discuss. Faraday Soc.*, **No. 47**, 93 (1969); C. H. Wei and L. F. Dahl, *Inorg. Chem.*, **6**, 1229 (1967); C. E. Strouse and L. F. Dahl, *J. Am. Chem. Soc.*, **93**, 6032 (1971); D. L. Stevenson, C. H. Wei, and L. F. Dahl, *ibid.*, **93**, 6027 (1971); (b) L. Markó, G. Bor, E. Klumpp, B. Markó, and G. Almásy, *Chem. Ber.*, **96**, 955 (1963). (c) Related oxygen complex of Re; G. Ciani, A. Sironi, and V. G. Albano, *J. Chem. Soc., Dalton Trans.*, 1667 (1977); A. Bertolucci, M. Freni, P. Romiti, G. Ciani, A. Sironi, and V. G. Albano, *J. Organomet. Chem.*, **113**, C61 (1976).
(24) S. Otsuka, A. Nakamura, and T. Yoshida, *Inorg. Chem.*, **7**, 261 (1968); N. Kamijyo and T. Watanabé, *Bull. Chem. Soc. Jpn.*, **47**, 373 (1974).
(25) B. H. Robinson, private communication. The original assignment (B. M. Peake, B. H. Robinson, J. Simpson, and D. J. Watson, *Inorg. Chem.*, **16**, 405 (1977)) was to an orbital of a_1 symmetry.
(26) G. L. Geoffroy and R. A. Epstein, *Inorg. Chem.*, **16**, 2795 (1977).
(27) (a) $Fe_3(CO)_9As_2$: L. T. J. Delbaere, L. J. Kruczynski, and D. W. McBride, *J. Chem. Soc., Dalton Trans.*, 307 (1973). (b) $Fe_3(CO)_9(AsPh)_2$: M. Jacob and E. Weiss, *J. Organomet. Chem.*, **131**, 263 (1977); G. Huttner, G. Mohr, A. Frank, and U. Schubert, *ibid.*, **118**, C73 (1976). (c) $Fe_3(CO)_9(Sn-(CpFe(CO)_2)_2$: T. J. McNeese, S. S. Wreford, D. L. Tipton, and R. Bau, *J. Chem. Soc., Chem. Commun.*, 390 (1977). (d) $Fe_3(CO)_9(NSi(CH_3)_3)$: B. L. Barnett and C. Kruger, *Angew. Chem.*, **83**, 969 (1971).
(28) (a) H. Vahrenkamp, V. A. Uchtman, and L. F. Dahl, *J. Am. Chem. Soc.*, **90**, 3272 (1968); (b) V. A. Uchtman and L. F. Dahl, *ibid.*, **91**, 3763 (1969); (c) P. D. Frisch and L. F. Dahl, *ibid.*, **94**, 5082 (1972).
(29) $Ni_3Cp_3(CO)_2$ is known (a) O. S. Mills, A. A. Hock, and G. Robinson, XVIIth International Congress of Pure and Applied Chemistry, Munich, 1959, p 143. Abstract: A. A. Hock and O. S. Mills, *Proc. Int. Conf. Coord. Chem.*,

6th, 640 (1961). (b) E. O. Fischer and C. Palm, *Chem. Ber.,* **91,** 1725 (1958).

(30) For a review see J. Lewis and B. F. G. Johnson, *Pure Appl. Chem.,* **44,** 43 (1975); A. J. Deeming, S. Hasso, and M. Underhill, *J. Chem. Soc., Dalton Trans.,* 1614 (1975); W. G. Jackson, B. F. G. Johnson, J. W. Kelland, J. Lewis, and K. T. Schorpp, *J. Organomet. Chem.,* **87,** C27 (1975); A. J. Canty, A. J. P. Domingos, B. F. G. Johnson, and J. Lewis, *J. Chem. Soc., Dalton Trans.,* 2056 (1973); see also ref 20. An isoelectronic nitrile cluster has the same perpendicular structure. See ref 22b and A. M. Andrews, C. B. Knobler, and M. D. Kaesz, to be published.

(31) Similar orientations are found in the formally isoelectronic HFe₃(CO)₉-(CH₃CNH) (ref 22b) and HOs₃(CO)₉(HCNPh): R. D. Adams and N. M. Golembeski, *J. Am. Chem. Soc.,* **100,** 4622 (1978). See also M. I. Bruce and R. C. Wallis, *J. Organomet. Chem.,* **164,** C6 (1979).

(32) (a) For a detailed analysis see B. E. R. Schilling, Ph.D. Dissertation, Cornell University. (b) B. E. R. Schilling and R. Hoffmann, *Acta Chem. Scand.,* in press.

(33) (a) M. Evans, M. Hursthouse, E. W. Randall, E. Rosenberg, L. Milone, and M. Valle, *J. Chem. Soc., Chem. Commun.,* 545 (1972); (b) M. I. Bruce, M. A. Cairns, A. Cox, M. Green, M. D. H. Smith, and P. Woodward, *Chem.*

Commun., 735 (1970); A. Cox and P. Woodward, *J. Chem. Soc. A,* 3599 (1971); (c) A. W. Parkins, E. O. Fischer, G. Huttner, and D. Regler, *Angew. Chem.,* **82,** 635 (1970). (d) NMR results suggesting the allylic structure: O. Gambino, M. Valle, S. Aime, and G. A. Vaglio, *Inorg. Chem. Acta,* **8,** 71 (1974). (e) G. Gervasio, *J. Chem. Soc., Chem. Commun.,* 25 (1976).

(34) E. G. Bryan, B. F. G. Johnson, J. W. Kelland, J. Lewis, and M. McPartlin, *J. Chem. Soc., Chem. Commun.,* 254 (1976).

(35) L. J. Farrugia, J. A. K. Howard, P. Mitrprachachon, J. L. Spencer, F. G. A. Stone, and P. Woodward, *J. Chem. Soc., Chem. Commun.,* 260 (1978).

(36) (a) D. M. P. Mingos, *J. Chem. Soc., Dalton Trans.,* 602 (1977); (b) P. Hofmann, *Angew Chem.,* **89,** 551 (1977); (c) ref 1e and 10.

(37) (a) D. M. P. Mingos, M. I. Forsyth, and A. J. Welch, *J. Chem. Soc., Dalton Trans.,* 1363 (1978), and references cited therein; (b) T. A. Albright and R. Hoffmann, *Chem. Ber.,* **111,** 1578 (1978).

(38) (a) J. D. Edwards, J. A. K. Howard, S. A. R. Knox, V. Riera, F. G. A. Stone, and P. Woodward, *J. Chem. Soc., Dalton Trans.,* 75 (1976); (b) M. R. Churchill, F. R. Scholer, and J. Wormald, *J. Organomet. Chem.,* **28,** C21 (1971); M. R. Churchill and J. Wormald, *Inorg. Chem.,* **12,** 191 (1973).

(39) R. Hoffmann, *J. Chem. Phys.,* **39,** 1397 (1963); R. Hoffmann and W. N. Lipscomb, *ibid.,* **36,** 2179, 3489 (1962); **37,** 2872 (1962).

Metal–Rare Gas Interaction. A New Bond?

J. Demuynck,* E. Kochanski, and A. Veillard

Contribution from the E. R. No. 139 du CNRS, Université L. Pasteur, 67000 Strasbourg, France. Received December 14, 1978

Abstract: The interaction between the pentacarbonyls $M(CO)_5$ (M = Cr and Mo) and a rare-gas atom X (X = Ar, Kr, Xe) has been studied through ab initio calculations both at the SCF level and at the level of the dispersion energy. The SCF calculations were carried out with two different basis sets, the largest one being of double-ζ quality. The interaction at the SCF level was attractive with the small basis set but repulsive with the large one. This repulsive character of the interaction at the SCF level has been discussed in terms of (1) the donor ability of the rare gas; (2) the existence of a destabilizing π interaction together with a stabilizing σ interaction; (3) the steric requirements of the rare gas. The dispersion energy in $Mo(CO)_5Kr$ has been estimated on the basis of a perturbation treatment for MoKr. This produces for the stabilization energy of $Mo(CO)_5Kr$ a value of 2.5 kcal/mol; however, this result is certainly underestimated and the exact value may be as high as 8–10 kcal/mol.

Introduction

Turner and his collaborators have reported that, in the UV–visible spectra of the matrix-generated pentacarbonyls $M(CO)_5$ (M = Cr, Mo, and W), the position of the visible band is extraordinarily sensitive to the matrix material used.[1] This band, which corresponds to the symmetry-allowed $^1A_1 \rightarrow {}^1E$ ($d_{xy}^2 d_{xz}^2 d_{yz}^2 \rightarrow d_{xy}^2 d_{xz}^{3/2} d_{yz}^{3/2} d_{z^2}^1$) transition is shifted from 624 nm in a Ne matrix to 490 nm in a Xe matrix. This observation together with the spectra in a mixed matrix and the dependence of the IR spectra with the matrix was interpreted by assuming that $Cr(CO)_5$, a square pyramid,[2-6] forms a weak bond with a rare-gas atom.[1] This weak bond corresponds to a stereospecific interaction via the vacant coordination site as shown in **1**. Perutz and Turner stated that the

1   **2**
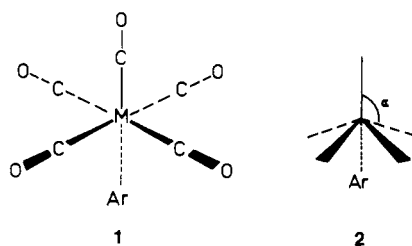
interaction energy between $Cr(CO)_5$ and a Xe atom occupying its vacant site might be comparable in energy to a weak chemical bond, namely, in the range 1–5 kcal/mol. Two possible explanations (or a combination of both) were given for the shift in the visible spectrum: (1) The rare-gas atom behaves as a weak σ donor through a σ lone pair (the np_z orbital of the rare gas if z is the rare gas–metal axis) which interacts with

the a_1 orbital (mostly a metal $3d_{z^2}$ orbital). This raises the a_1 orbital in energy (Figure 1), thus increasing the e $\rightarrow a_1$ transition energy. (2) Small changes in the axial-radial bond angle α of $M(CO)_5$ (**2**) are induced by the rare-gas atom in the vacant coordination site with the energy of the orbital a_1 falling rapidly when α increases. Thus a small increase in α can generate a large decrease in the e $\rightarrow a_1$ energy. Subsequently Turner and his collaborators have reported that "Fe(CO)₄ reacts with the matrix to form Fe(CO)₄Xe";[7] their statement implies the formation of a new species with a rare gas–metal bond (both $Cr(CO)_5$ and $Fe(CO)_4$ are 16-electron species).

The ability of the rare gases to enter into chemical combination with other atoms is very limited and so far compounds of Kr and Xe have been reported only with the most electronegative elements.[8] For this reason, we considered it worthwhile to investigate, through ab initio calculations, the nature of the interaction between $M(CO)_5$ and a rare gas. Through these ab initio calculations we have sought some answers to the following questions: (1) Is the interaction of the donor–acceptor type, namely, is it a dative bond involving a lone pair of the rare-gas atom and the vacancy on $M(CO)_5$, as postulated initially by Turner,[1] or is the interaction of the van der Waals type with the dispersion energy representing the predominant contribution? (2) Is the interaction energy large enough that one can speak of a metal–rare gas bond or is it merely a weak interaction of the type found in many van der Waals complexes? The borderline between the chemical bond and molecular interactions is a loose one. Rather arbitrarily we would put the border between a "weak interaction" and a "chemical bond" at 5 kcal/mol; however, we agree that the distinction is rather arbitrary.[9]